

**Final Report on key Comparison  
between TUBITAK UME and VNIIM  
COOMET.M.P-K15 (711/TR/16)  
in the pressure range from  $3 \cdot 10^{-4}$  Pa to 0.9 Pa**

*Rifat Kangi<sup>1</sup>, Alper Elkatmis<sup>1</sup>, Aleksandr Chernyshenko<sup>2</sup>*

*April 2023*

---

<sup>1</sup> TUBITAK UME, TUBITAK Gebze Yerleskesi, P.K. 54, 41470 Gebze / KOCAELI, Türkiye

<sup>2</sup> D.I. Mendeleyev Institute for Metrology (VNIIM), 19 Moskovsky pr., St.Petersburg, 190005 Russia

## Content

Page number

1. Introduction.....	3
2. Participating laboratories and their standards .....	3
2.1. The UME static expansion system.....	4
2.2. The VNIIM Combined compensation type membrane-capacitance manometer and continuous expansion system .....	5
3. Transfer standards .....	6
4. Calibration constant .....	6
5. Organisation of the comparison and schedule .....	7
6. Calibration procedure and reported results .....	8
7. Uncertainties of primary standards .....	9
8. Uncertainties of reported measured values .....	9
9. Reported results of the laboratories .....	11
10. Stability of Transfer gauges .....	14
11. Data reduction and evaluation of the degree of equivalence .....	14
12. Discussion and conclusions .....	19
13. References.....	20

## 1. Introduction

The purpose of the comparison is to confirm the required level of accuracy for pressure measurements and to ensure the uniformity of low absolute pressure measurements in the participating countries.

The objective of the comparison is therefore to comply with the requirement by the determination of the relative agreement between the absolute pressure standards of UME and VNIIM via the effective accommodation factor  $\sigma_{\text{eff}}$  using transfer standard spinning rotor gauge (SRG).

Two spinning rotor gauges (SRG) were characterised with the pressure standards of each participating institute in the range from 0.3 mPa to 0.9 Pa. From these measurements, the accommodation factor of the SRG was determined at each measurement point by which the generated pressures in the standards could be compared.

The transfer standard package consisted of one spinning rotor gauge (SRG). This gauge was equipped with transportation mechanism which allowed the rotor to travel in a fixed position under vacuum. Another gauge without a transport mechanism was provided by VNIIM. For the purposes of this bi-lateral comparison UME acted as the pilot laboratory.

Comparison measurements at UME and VNIIM were performed simultaneously for the two spinning rotor gauges, each being operated by a MKS SRG2 controller with a SH-700 sensing head.

Data was collected and analysed according to the protocol of the COOMET.M.P-K15 [1] that was completed between October 2016 and December 2018.

At both UME and VNIIM, the measurements were performed on consecutive days using the standards described below. The following target pressures were used for the calibration:  $3 \cdot 10^{-4}$  Pa,  $9 \cdot 10^{-4}$  Pa,  $3 \cdot 10^{-3}$  Pa,  $9 \cdot 10^{-3}$  Pa,  $3 \cdot 10^{-2}$  Pa,  $9 \cdot 10^{-2}$  Pa, 0.3 Pa and 0.9 Pa.

The report begins with a brief description of the vacuum standards used and their principle of operation. The measurements are then described and summarised. Finally, the evaluation of various uncertainty estimates is explained.

## 2. Participating laboratories and their standards

Table 1 Details of participating standards.

Laboratory	Standard	Definition	Traceability	CMC
UME	Static expansion system	Primary	Independent	Yes
VNIIM	1. Compensation type membrane-capacitance manometer	Primary	Independent	Yes
	2. Continuous expansion system	Primary	Independent	Yes

## 2.1. The UME static expansion system

The UME series expansion system MSSE1 used for this comparison is independent primary standard which is shown schematically below.

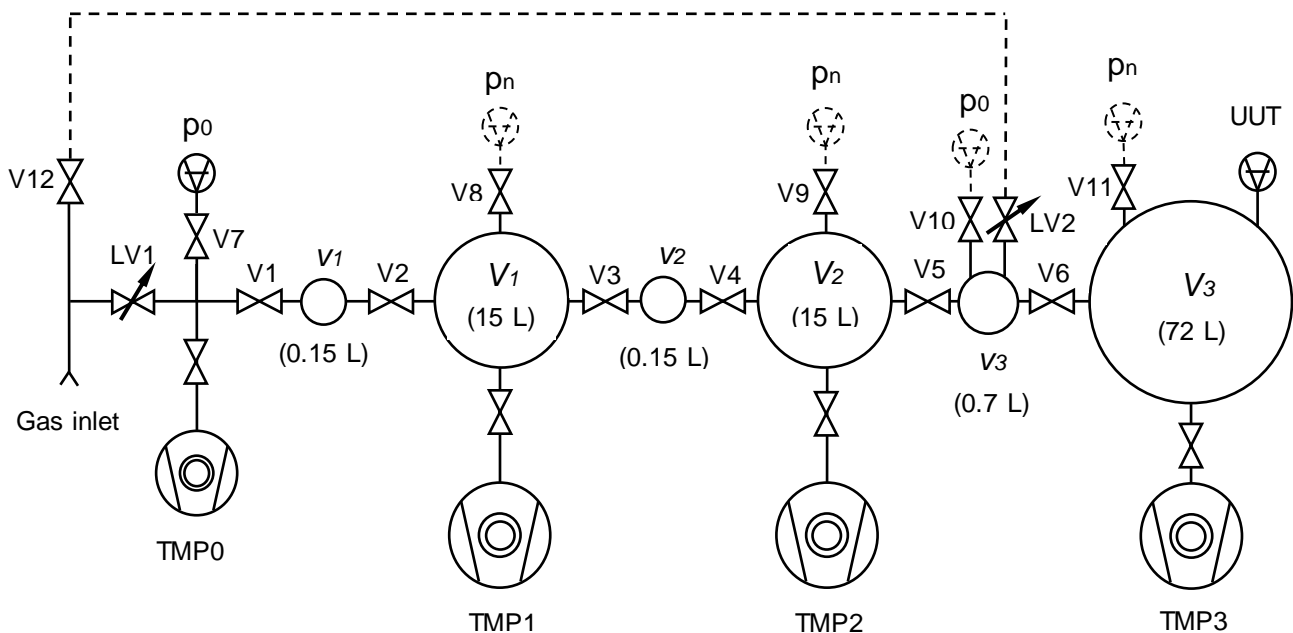


Figure 1 Schematic representation of the series expansion system MSSE1

Using this apparatus, calculable pressures between  $3 \cdot 10^{-4}$  Pa and  $1 \cdot 10^3$  Pa may be generated using the series expansion method.

In operation, a sample of gas is contained in one of the small vessels (i.e.  $v_1$ ,  $v_2$  or  $v_3$ ) and then expanded into the next large and small vessels, which have been previously evacuated to a high vacuum. This procedure is then repeated using subsequent expansion stages until the gas is expanded into the calibration vessel ( $V_3$ ). To generate pressure in the lowest range, the gas expands from the small vessel  $v_1$  to the large vessel  $V_1$  and the small vessel  $v_2$  twice (cascade method). The pressure of the initial gas sample is measured using a calibrated resonant silicon gauge. By varying the initial pressure and the number of expansion stages, a range of pressures may be generated in the calibration vessel. The pressure generated is calculated from knowledge of the initial pressure, the gas temperature and the ratio of the relevant volumes. The system is described in more detail in reference [2].

## 2.2. The VNIIM Combined compensation type membrane-capacitance manometer and continuous expansion system

The VNIIM's pressure standard (GET 49-2016) is based on the two methods: continuous expansion method and on the method of compensation of pressure by capacitance diaphragm manometer. Continuous expansion system is used to measure medium and high vacuum within the range of  $1 \cdot 10^{-4}$  Pa to  $1 \cdot 10^{-2}$  Pa absolute pressure. The VNIIM's continuous expansion system is based on the expansion of pure gas, which is pumped through a fixed conductance. The effective pumping speed is computed from the values of calculated conductance and the ratio of the conductance to the pumping speed is periodically measured. The expanded ( $k = 2$ ) uncertainties of pressures generated by this system range from  $6 \cdot 10^{-6}$  to  $5 \cdot 10^{-4}$  Pa.

To generate absolute pressure in the medium and high vacuum range within of  $1 \cdot 10^{-2}$  Pa to 10 Pa compensation type capacitance diaphragm manometer system has been used. Compensation principle, based on balancing between the pressure force and electrostatic force acting on the plates of flat capacitor. The expanded ( $k = 2$ ) uncertainties of pressures generated by this standard range from  $5 \cdot 10^{-4}$  to 0.14 Pa. The system is described in more detail in reference [3].

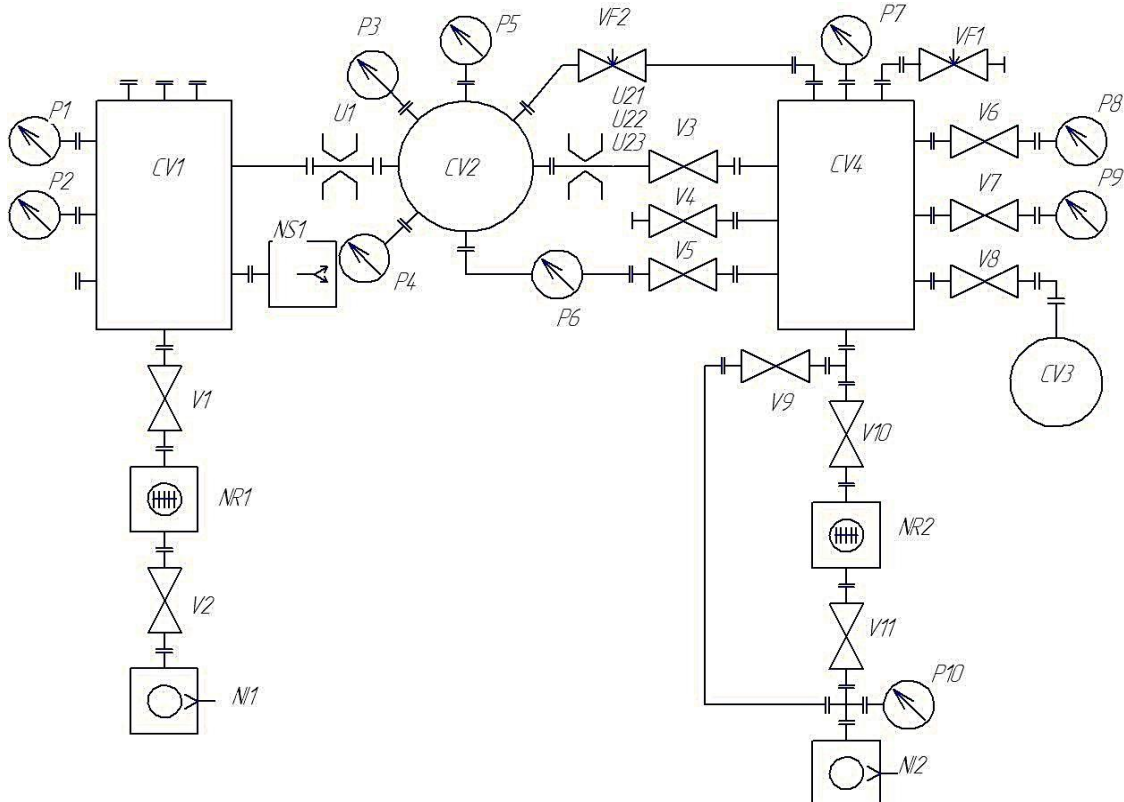


Figure 2 Schematic representation of the VNIIM vacuum standard.

### 3. Transfer standards

The spinning rotor gauge is widely accepted as a transfer standard due to its measurement accuracy and long-term and transport stability. Two devices were used in order to reduce the influence of transport instabilities, to provide redundancy and to increase the accuracy of the comparison. One of the spinning rotor gauges (SRG) was supplied by UME and other by VNIIM. Each laboratory used its own controllers.

The details of the two spinning rotor gauges used as transfer standards are shown in Table 2.

Table 2 Transfer standards used for comparison.

<b>Transfer Standard #1</b>	Spinning Rotor Gauge (SRG)
Manufacturer	MKS
Part Number	SRG1
Measuring head	SRG-SH 700-V3
Serial Number	G94377G60
Ball Diameter (Nominal)	4.5 mm
Ball Density (Nominal)	7715 kg/m <sup>3</sup>
Rotation Frequency	Min: 430 Hz Max: 440 Hz
Valve Manufacturer	NA
Valve Serial Number	NA
Volume, Valve Open	NA
<b>Transfer Standard #2</b>	Spinning Rotor Gauge (SRG)
Manufacturer	MKS
Part Number	SRG2
Measuring head	SRG-SH 700
Serial Number	192338
Ball Diameter (Nominal)	4.5 mm
Ball Density (Nominal)	7715 kg/m <sup>3</sup>
Rotation Frequency	Min: 430 Hz Max: 440 Hz
Valve Manufacturer	Varian
Valve Serial Number	NA
Volume, Valve Open	NA

### 4. Calibration constant

The value to be calibrated by each laboratory  $j$  for each pressure and for each rotor  $i$  was the effective accommodation coefficient  $\sigma_{ij}$ , often called  $\sigma_{eff}$ , which is mainly determined by the tangential momentum accommodation coefficient of the gas molecules to the rotor, and partly by the energy accommodation factor and additionally by using nominal values for diameter and density of the rotors instead of the real ones [4].

$\sigma_{ij}$  was determined by the following equation:

$$\sigma_{ij} = \sqrt{\frac{8kT_j}{\pi m} \frac{\pi d_i \rho_i}{20 p_{stj}} \left( \left( \frac{\dot{\omega}}{\omega} \right)_i - RD_i(\omega) \right)} \quad (1)$$

where:

$p_{st}$  = is the generated pressure in the standard

$T_j$  = the temperature of the gas in the calibration vessel

$d_i$  = the nominal diameter of the rotor  $i$

$\rho_i$  = the nominal density of the rotor  $i$

$m$  = the molecular mass of nitrogen

$(\dot{\omega}/\omega)_i$  = the relative deceleration rate of the rotor frequency  $\omega$  (DCR)

$RD_i$  = pressure independent residual drag

$RD$  is a function of  $\omega$ ,  $RD(\omega)$ , so whenever a determination of  $\sigma_{ij}$  is made it was necessary to measure the value of  $\omega$  in order to subtract the correct  $RD(\omega)$  in Eq.(1).

Participants used the same approach for measuring  $RD(\omega)$ .

Before starting the calibrations the rotor frequency dependence of the residual drag (in units  $DCR = s^{-1}$ ) was measured over a long period of time. Furthermore, before each of the two calibration cycles of each rotor, the behaviour of the offset signal was checked to verify that it was comparable with the estimate of  $RD(\omega)$  obtained by the previous “long” acquisition. The rotor frequency covered the full range that may occur during the calibration. Linear least square fit was applied to obtain the function  $RD(\omega)$ .

## 5. Organisation of the comparison and schedule

Two spinning rotor gauges were used as transfer standards as described in Section 3. The initial calibration was performed at UME in October 2016. Initially, during the first measurement at UME in 2016, the UME rotor (named SRG3) was used as rotor 2, but due to its instability it was replaced by another UME rotor (named SRG6) and used in the following measurements conducted at VNIIM and UME in 2018. Measurements were taken for two days and with two measurements at each pressure point. Then the UME SRG, equipped with a transport mechanism that allows the rotor to be transported in a fixed position and under vacuum, was delivered by courier to VNIIM. The second calibration was performed at VNIIM in June 2018.

Two SRGs were used in these measurements. Measurements were taken for two days and with two measurements at each pressure point. The final calibration was performed at UME in December 2018. Two SRGs were used in these measurements. VNIIM SRG was brought with him during the visit of colleagues from VNIIM to UME. Measurements were taken for two days and with two measurements at each pressure point.

To monitor any transport instability, a third spinning rotor gauge (check standard) was calibrated by UME at the same time as the transfer gauges. It was not removed from the UME primary standard throughout the duration of the comparison.

Table 3 The chronology of the calibrations is shown below.

No.	Period of Measurements	NMIs
1	October, 2016 (1 SRG)	UME
2	June, 2018 (2 SRGs)	VNIIM
3	December, 2018 (2 SRGs)	UME

## 6. Calibration procedure and reported results

The calibration procedure agreed upon before the comparison was similar to that of the EURAMET.M.P-K15.1 key comparison [5]: Each laboratory calibrated the two SRGs at 8 nominal target pressures  $p_t$  for nitrogen pressure in ascending order: 0.3 mPa, 0.9 mPa,  $3 \cdot 10^{-3}$  Pa,  $9 \cdot 10^{-3}$  Pa,  $3 \cdot 10^{-2}$  Pa,  $9 \cdot 10^{-2}$  Pa, 0.3 Pa, 0.9 Pa.

A tolerance of  $\pm 10\%$  in establishing the nominal pressure was accepted for  $p_t < 9 \cdot 10^{-2}$  Pa and  $\pm 5\%$  for  $9 \cdot 10^{-2}$  Pa. Each target pressure had to be generated 2 times. After a measurement at the target point, the system was pumped down to residual pressure conditions and the same point re-generated. In total 16 measurements were made in each calibration sequence. It was required that this calibration sequence be repeated at least once on another day.

The number of readings and sample interval times for each point were as follows:

- 5 repeat points at 30 s intervals for the target points  $3 \cdot 10^{-4}$  Pa,  $9 \cdot 10^{-4}$  Pa, and  $3 \cdot 10^{-3}$  Pa.
- 3 repeat points at 30 s intervals for  $9 \cdot 10^{-3}$  Pa,  $3 \cdot 10^{-2}$  Pa,  $9 \cdot 10^{-2}$  Pa.
- 3 repeat points at 10 s intervals for 0.3 Pa and 0.9 Pa.

It was required that the offset be measured during the calibration no matter what method had been chosen for offset determination:

It was agreed that no bake-out should be performed as part of the calibration sequence since it is both time consuming and may also affect the accommodation coefficient.

At the end of this calibration procedure, for each generated  $p_{stj}$  near the respective target point and for each rotor  $i$  and for each of the calibration sequences a value for  $\sigma_{ij}$  existed. Together with the value of  $\sigma_j$ , each laboratory also reported the standard uncertainty  $u(p_{stj})$  of  $p_{stj}$ .

## 7. Uncertainties of primary standards

Table 4 shows the relative standard uncertainties due to Type B uncertainties for the two primary standards. Type A uncertainties of the standards will be incorporated in the scatter of data for repeat measurements.

Table 4 Relative standard uncertainties of generated pressures due to systematic effects (Type B) as reported by participants.

$p_{st}$ (Pa)	UME	VNIIM
3.00E-04	2.7E-3	2.8E-2
9.00E-04	2.7E-3	2.9E-2
3.00E-03	2.2E-3	2.6E-2
9.00E-03	2.1E-3	2.9E-2
3.00E-02	2.1E-3	3.0E-2
9.00E-02	2.1E-3	2.7E-2
3.00E-01	1.6E-3	1.7E-2
9.00E-01	1.8E-3	6.5E-3

## 8. Uncertainties of reported measured values

Again, following the analysis of key comparison EURAMET.M.P-K15.1 [5], we introduce:

$$K_i = \sqrt{\frac{8k \cdot 293.15}{\pi m} \frac{\pi d_i \rho_i}{20}}, \quad (2)$$

and

$$DCR_i = \left(\frac{\dot{\omega}}{\omega}\right)_i \quad (3)$$

The effective accommodation coefficient has been measured  $n = 4$  times  $\sigma_{ijk}$ ,  $k=1 \dots n$ , therefore we can write:

$$\sigma_{ijk} = \sqrt{\frac{T_{jk}}{293.15}} \cdot \frac{K_i}{p_{stjk}} (DCR_{ik} - RD_{ik}(\omega)) \quad (4)$$

and Eq. (1) can be replaced by taking the mean of the repeated measurements to give

$$\sigma_{ij} = \frac{1}{n} \sum_{k=1}^n \sigma_{ijk} \quad (5)$$

The same values for  $k$ ,  $m$ ,  $d_i$ , and  $\rho_i$  were used by each laboratory and the  $K_i$  were therefore fully correlated, so that in effect no uncertainty needed to be attributed to  $K_i$  (a systematic error in  $d_i$  for example, would be calibrated into  $\sigma_{ij}$  in the same way at each laboratory and would have no effect on the result of the comparison). All type A uncertainties of values on the right hand side of Eq. (4) will contribute to the scatter of  $\sigma_{ijk}$  and hence the standard deviation of  $\sigma_{ij}$ . Therefore since Type A uncertainties are accounted for by the standard deviation, for calculation of the overall uncertainty of  $\sigma_{ij}$  only the type B uncertainties of values on the right hand side of Eq. (4) have to be evaluated for inclusion. For  $DCR_i$  there is no such uncertainty.  $RD(\omega)$  is not determined at the same time as  $DCR_i$ , but before or after the measurement, and so therefore has a Type B uncertainty. Also the gas temperature and the generated pressure  $p_{stj}$  will have Type B uncertainties which are known before the measurements.

For this reason the variance in  $\sigma_{ij}$  is given by:

$$u_{\sigma_{ij}}^2 = \frac{n-1}{n-3} s_{\sigma_{ij}}^2 + \left[ \frac{\partial \sigma_{ij}}{\partial RD_i} \right]^2 u_{RD_i}^2 + \left[ \frac{\partial \sigma_{ij}}{\partial T_j} \right]^2 u_{T_j}^2 + \left[ \frac{\partial \sigma_{ij}}{\partial p_{stj}} \right]^2 u_{p_{stj}}^2, \quad (6)$$

where  $s_{\sigma_{ij}}^2$  is the square of the standard deviation of the mean of the repeat measurements  $\sigma_{ijk}$  and where we understand that all standard uncertainties  $u$  are due to systematic effects which do not contribute to the scatter of  $\sigma_{ij}$ . Since only 4 measurements were taken, the square root of  $s_{\sigma_{ij}}^2$  was multiplied by 1.73 for  $n=4$  as suggested by Kacker and Jones [6]:

The last term in Eq. (6) is due to the generated pressure as described in section 7, all other terms are due to uncertainties of the transfer standard.

The sensitivity coefficients are:

$$\left( \frac{\partial \sigma_{ij}}{\partial RD_i} \right) = - \frac{K_i}{p_{stj}} \cdot \sqrt{\frac{T_j}{293.15}} \quad (7)$$

$$\left( \frac{\partial \sigma_{ij}}{\partial p_{stj}} \right) = - \frac{K_i}{p_{stj}^2} \cdot \sqrt{\frac{T_j}{293.15}} (DCR_i - RD_i) \quad (8)$$

$$\left(\frac{\partial \sigma_{ij}}{\partial T_j}\right) = \frac{1}{2} \frac{K_i}{p_{stj}} \cdot \frac{1}{\sqrt{293.15}} \cdot \frac{1}{\sqrt{T_j}} (DCR_i - RD_i) \quad (9)$$

$u(p_{stj})$  and  $u(T_j)$  were reported by each laboratory, where it is assumed that  $T_{jk} \approx T_j$  (constant temperature of standard during 2 repeat measurements). The following effects may contribute to the uncertainty of the residual drag  $RD$ :

- the scatter of the measurement results,
- the imprecisely known frequency dependence of the offset,
- a possible drift of the offset values between its determination and the time of calibration,

## 9. Reported results of the laboratories

As UME had carried out two calibration sequences and VNIIM one, it was possible to check to see if a significant change could be observed between  $\sigma_j$  for each sequence.

No shift in the mean  $\sigma_j$  value was seen at UME between the results collected in October 2016 and December 2018 for both of the spinning rotor gauges used as transfer standards.

Therefore the mean value of all data for a single rotor at a single target pressure could be taken for data reduction:

$$\sigma_{ij} = \frac{1}{n} \sum_{k=1}^n \sigma_{ijk} \quad n = 4 \quad (5)$$

The results reported by each laboratory and the corresponding uncertainties according to Eq, (6) are shown in the following Tables and Figures.

Table 5 The mean values  $\sigma_j$  of the reported results for Rotor 1 (VNIIM) and the uncertainties as calculated by Eq.(6).

$P_t / Pa$	UME 1		VNIIM		UME 2	
	$\sigma_1$	$u(\sigma_1)$	$\sigma_1$	$u(\sigma_1)$	$\sigma_1$	$u(\sigma_1)$
3.00E-04	1.1930	0.0084	0.9779	0.0324	0.9925	0.0142
9.00E-04	1.0373	0.0044	0.9677	0.0230	0.9891	0.0056
3.00E-03	1.0020	0.0027	1.0183	0.0149	0.9840	0.0027
9.00E-03	0.9856	0.0025	1.1026	0.0176	0.9843	0.0023
3.00E-02	0.9794	0.0017	0.9695	0.0149	0.9842	0.0022
9.00E-02	0.9772	0.0024	0.9716	0.0141	0.9835	0.0022
3.00E-01	0.9731	0.0019	0.9672	0.0089	0.9785	0.0017
9.00E-01	0.9617	0.0021	0.9593	0.0041	0.9682	0.0019

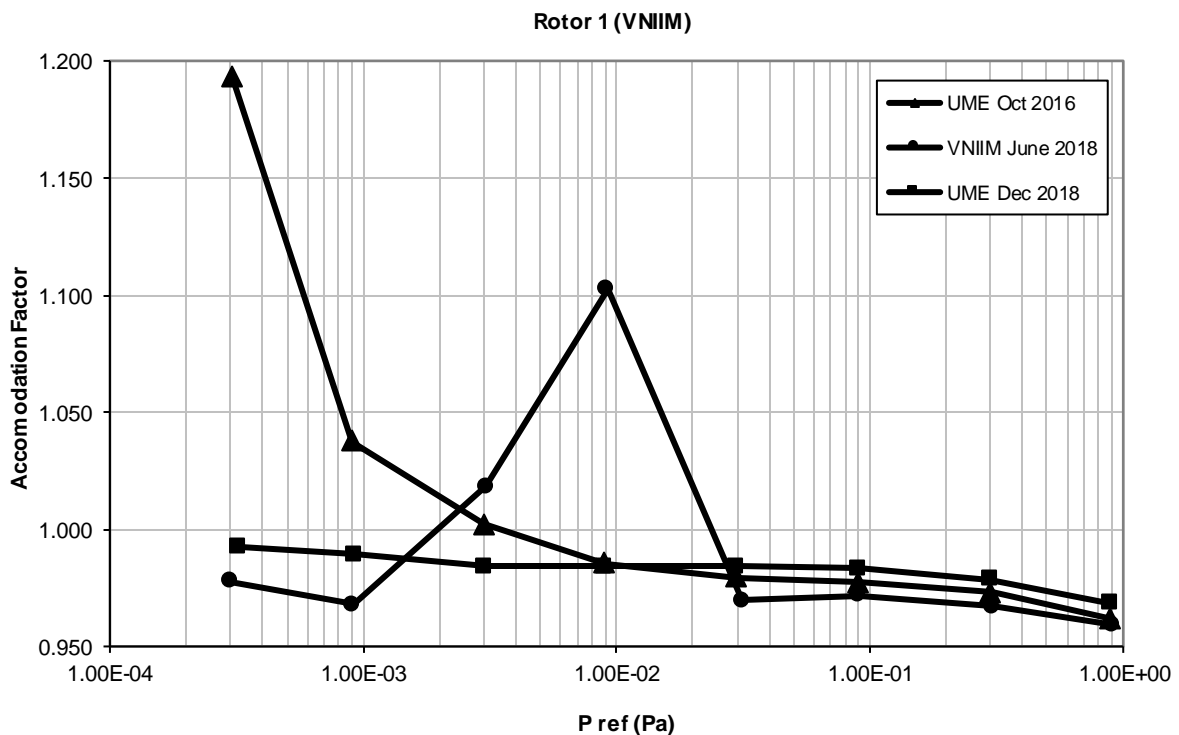


Figure 3 Graphical presentation of the results of Rotor 1 (Table 5). Uncertainties are not shown for better visibility and can be taken from table 5.

Table 6 The mean values  $\sigma_2$  of the reported results for Rotor 2 (UME) and the uncertainties as calculated by Eq.(6).

$P_t / Pa$	UME 1		VNIIM		UME 2	
	$\sigma_2$	$u(\sigma_2)$	$\sigma_2$	$u(\sigma_2)$	$\sigma_2$	$u(\sigma_2)$
3.00E-04	-	-	0.9831	0.0554	0.9717	0.0142
9.00E-04	-	-	0.9652	0.0382	0.9767	0.0056
3.00E-03	-	-	1.0149	0.0167	0.9719	0.0027
9.00E-03	-	-	1.0979	0.0197	0.9724	0.0023
3.00E-02	-	-	0.9652	0.0149	0.9725	0.0022
9.00E-02	-	-	0.9672	0.0140	0.9718	0.0022
3.00E-01	-	-	0.9627	0.0089	0.9671	0.0017
9.00E-01	-	-	0.9546	0.0041	0.9571	0.0019

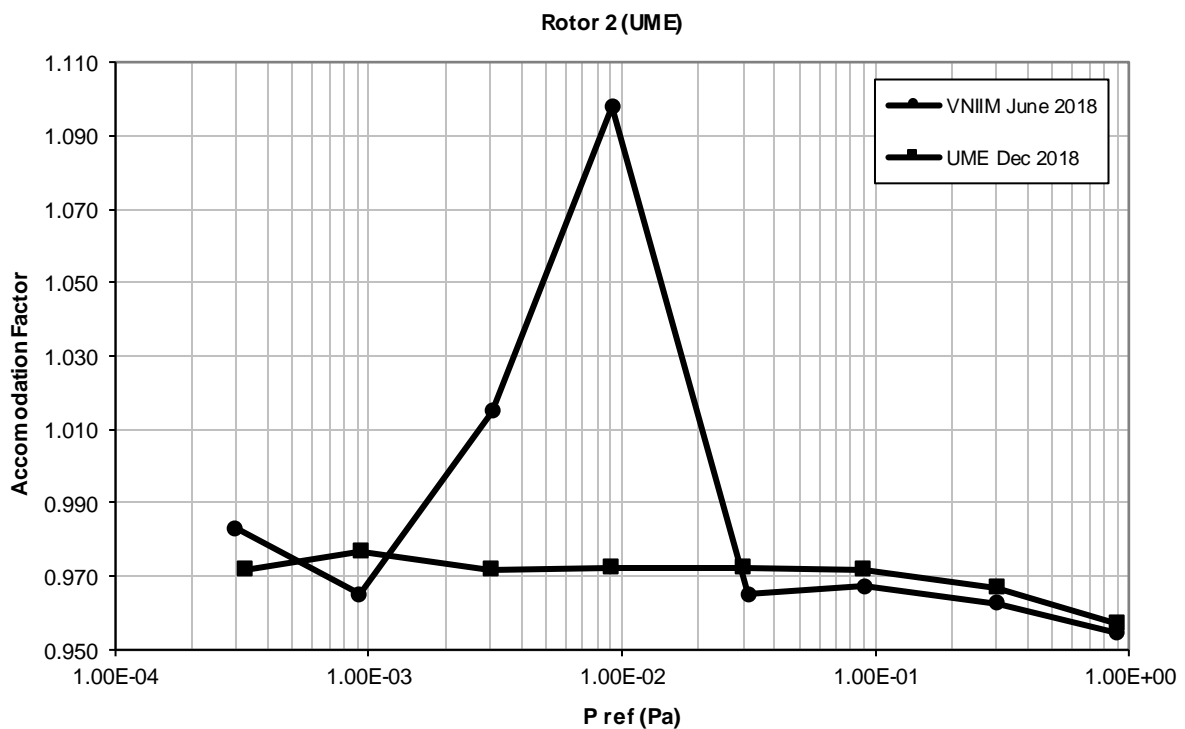


Figure 4 Graphical presentation of the results of Rotor 2 (UME) (Table 6). Uncertainties are not shown for better visibility and can be taken from table 6.

The results show that the values for both rotors obtained at VNIIM at pressures  $3 \cdot 10^{-3}$  Pa and  $9 \cdot 10^{-3}$  Pa are systematically higher than those measured at UME. The first results for rotor 1,

obtained at UME at pressures  $3 \cdot 10^{-4}$  Pa and  $9 \cdot 10^{-4}$  Pa are also significantly higher than the results measured at VNIIM and the latest measurements at the UME. In Table 5, UME measurements less than  $9 \cdot 10^{-3}$  Pa in 2016 can be explained by a leak, but not for the VNIIM results, that was subsequently eliminated. The results in Table 6 confirm the major problem at VNIIM for the points  $3 \cdot 10^{-3}$  Pa and  $9 \cdot 10^{-3}$  Pa. Rotor 2, due to its instability, was replaced by another one (UME, named SRG6); the results of its measurements were removed from the calculations for 2016.

## 10. Stability of Transfer gauges

In order to monitor the transport stability of the calibration constant of the two rotors during the course of the comparison, the mean values of  $\sigma_1$  and  $\sigma_2$  between  $9 \cdot 10^{-4}$  Pa and  $3 \cdot 10^{-2}$  Pa of the pilot lab were calculated. Table 7 shows the results. Rotor 3 was the check standard that did not travel.

Table 7 The mean values of  $\sigma_1$  and  $\sigma_2$  between  $9 \cdot 10^{-3}$  Pa and  $9 \cdot 10^{-2}$  Pa for the two UME calibrations and the respective scatter (standard deviation  $s$ ) of the mean. Rotor 3 with the value  $\sigma_3$  did not travel and served as check standard for UME.

	$\sigma_1$	$s(\sigma_1)$	$\sigma_2$	$s(\sigma_2)$	$\sigma_3$	$s(\sigma_3)$
<b>UME1</b>	0.9807	0.004	-	-	0.9656	0.004
<b>UME2</b>	0.9840	0.0004	0.9722	0.0004	0.9635	0.003

Since the measured changes between UME1 and UME2 are within the standard deviation of each mean value, it is reasonable to assume that both effective accommodation coefficients did not change during this bilateral comparison.

## 11. Data reduction and evaluation of the degree of equivalence

Since the situation is similar to that given in the report [7], the analysis presented in that report can be followed. As outlined in the previous section, it is reasonable to assume that the transport instability of the two spinning rotor gauges was zero during this comparison. For this reason all values taken at the pilot laboratory UME can be assumed to belong to the same parent population and the mean of all this data can be taken.

$$\sigma_{ij} = \frac{1}{n} \sum_{k=1}^n \sigma_{ijk} \quad n = 8 \quad (10)$$

Since one of the goals of this comparison is to compare the generated pressures of the two standards, a pressure value has to be generated from the  $\sigma_{ij}$ .

For the data from each laboratory and for each spinning rotor gauge  $i$  a value of indicated pressure  $p_{ij}$  for a common hypothetical target pressure  $p_t$  can be calculated with the following equation:

$$p_{ij} = p_t \cdot \sigma_{ij} \quad i = 1,2 \quad j = 1,2 \quad (11)$$

$\sigma_{ij}$  denotes the mean accommodation coefficient according to Eq.(5) of spinning rotor gauge  $i$  as determined by VNIIM ( $j=1$ ) or according to Eq. (10) of SRG  $i$  as determined by UME ( $j=2$ ).

The method adopted here is to use  $\sigma_{ij}$  to predict gauge readings that would be observed when the different standards are set to generate pressures of the same value at a coincident time. The difference in the predicted gauge readings is taken as an indicator of the difference between the true pressures actually realised by the different standards (“generated pressures”) when the two laboratories state the same calculated value. This latter difference between calculated pressures, when the standards are set to produce exactly the same transfer gauge reading near the target pressure, is to a very good approximation (provided the differences are small) equal to the difference in the predicted gauge readings but of opposite sign.

It was found by Jousten [8] that  $\sigma_{ij}$  may be slightly temperature dependent. The size of this effect varies from rotor to rotor and is also dependent on the specific surface condition of a single rotor. Relative temperature changes of  $(\Delta\sigma_{eff} / \Delta T) / \sigma_{eff} = -1 \cdot 10^{-4} / \text{K}$  to  $-4 \cdot 10^{-4} / \text{K}$  were found around room temperature.

The mean temperatures during calibrations at UME (293.18 K) and VNIIM (293.86 K) differed by 0.67 K. Since the temperature dependence of  $\sigma_{eff}$  of the transfer standards was not measured and may also have changed during the comparison, the only possibility to consider this effect is to add an uncertainty for the  $p_{ij}$  in Eq. (11)

If we assume a mean temperature of 293.52 K so that each laboratory differs by 0.336 K from this temperature, and a possible temperature dependence of  $(\Delta\sigma_{eff} / \Delta T) / \sigma_{eff} = -2 \cdot 10^{-4} / \text{K}$  to calculate the standard uncertainty of the temperature effect for the  $p_{ij}$  in Eq. (11)

$$u_{T\sigma}(p_{ij}) = 0.67 \cdot 10^{-4} p_{ij} \quad (12)$$

Since  $p_t$  is simply a numerical value without uncertainty, the uncertainty of  $p_{ij}$  is calculated from the following equation:

$$u(p_{ij}) = p_{ij} \sqrt{\left(\frac{u(\sigma_{ij})}{\sigma_{ij}}\right)^2 + \left(\frac{u_{T\sigma}(p_{ij})}{p_{ij}}\right)^2} \quad (13)$$

$u(\sigma_{ij})$  was given in Eq. (6) and  $u_{T\sigma}(p_{ij})$  in Eq. (12)

The following tables show the results for the  $p_{ij}$  obtained from Eqs. (11) and (13).

Table 8 The predicted gauge readings and their uncertainties as obtained from Eqs. (11) and (13) for rotor 1.

$P_t$ (Pa)	$P_{1UME}$ (Pa)	$u(P_{1UME})$	$P_{1VNIIM}$ (Pa)	$u(P_{1VNIIM})$
3.0E-04	3.278E-04	3.383E-06	2.934E-04	9.735E-06
9.0E-04	9.119E-04	4.505E-06	8.709E-04	2.068E-05
3.0E-03	2.979E-03	8.209E-06	3.055E-03	4.282E-05
9.0E-03	8.864E-03	2.148E-05	9.923E-03	1.588E-04
2.0E-02	2.945E-02	5.822E-05	2.909E-02	4.467E-04
9.0E-02	8.823E-02	2.059E-04	8.744E-02	1.265E-03
3.0E-01	2.927E-01	5.388E-04	2.902E-01	2.678E-03
9.0E-01	8.685E-01	1.778E-03	8.634E-01	3.651E-03

Table 9 The predicted gauge readings and their uncertainties as obtained from Eqs. (11) and (13) for rotor 2.

$P_t$ (Pa)	$P_{2UME}$ (Pa)	$u(P_{2UME})$	$P_{2VNIIM}$ (Pa)	$u(P_{2VNIIM})$
3.0E-04	2.915E-04	4.256E-06	2.949E-04	1.662E-05
9.0E-04	8.790E-04	5.062E-06	8.687E-04	3.437E-05
3.0E-03	2.916E-03	8.208E-06	3.045E-03	5.024E-05
9.0E-03	8.752E-03	2.037E-05	9.881E-03	1.772E-04
2.0E-02	2.918E-02	6.617E-05	2.896E-02	4.470E-04
9.0E-02	8.746E-02	1.944E-04	8.705E-02	1.260E-03
3.0E-01	2.901E-01	5.099E-04	2.888E-01	2.669E-03
9.0E-01	8.614E-01	1.673E-03	8.591E-01	3.727E-03

The degree of equivalence between the two standards can be tested using [9]:

$$d_i = p_{iVNIIM} - p_{iUME} \quad (14)$$

for each target point and each transfer standard  $i$ . The uncertainty  $u(d_i)$  is given by

$$u(d_i) = \sqrt{u^2(p_{iVNIIM}) + u^2(p_{iUME})} \quad (15)$$

For a clear visualization of the results, the ratio was used, which is defined as:

$$r_i = \frac{p_{iVNIIM}}{p_{iUME}} \quad (16)$$

with

$$u(r_i) = \sqrt{\left(\frac{u(p_{iVNIIM})}{p_{iVNIIM}}\right)^2 + \left(\frac{u(p_{iUME})}{p_{iUME}}\right)^2} \quad (17)$$

Table 10 The ratios  $r_i = p_{iVNIIM}/p_{iUME}$  and their uncertainties as determined by Eqs. (16) and (17).

$P_t$ (Pa)	$r_1$	$r_2$	$u(r_1)$	$u(r_2)$	$u'(r_1)$	$u'(r_2)$
3.0E-04	0.8949	1.0117	0.0348	0.0777	0.0310	0.0761
9.0E-04	0.9551	0.9881	0.0243	0.0536	0.0184	0.0512
3.0E-03	1.0305	1.0442	0.0142	0.0189	0.0029	0.0128
9.0E-03	1.1195	1.1290	0.0162	0.0203	0.0049	0.0133
2.0E-02	0.9875	0.9925	0.0155	0.0157	0.0014	0.0028
9.0E-02	0.9911	0.9953	0.0147	0.0146	0.0011	0.0012
3.0E-01	0.9912	0.9955	0.0094	0.0094	0.0011	0.0013
9.0E-01	0.9941	0.9974	0.0047	0.0049	0.0012	0.0018

If  $r_1$  and  $r_2$  are of the approximate same value significantly different from 1, this would clearly indicate a difference in the true generated pressures of the two standards. Generally the values of  $r_1$  and  $r_2$  will be slightly different due to the scatter of the data.  $r_1$  and  $r_2$  are correlated, because the same standards  $j$  were used to determine  $\sigma_{1j}$  and  $\sigma_{2j}$ . In the appendix of reference [10] is outlined a way to consider this correlation by omitting  $u(p_{stj})$  in Eq.(6) for the determination of  $u(p_{ij})$  in Eq.(13). The respective value is called  $u'$  which is also listed in Table 10. The weighted mean  $r$  of  $r_1$  and  $r_2$  is then calculated for each target point by

$$r = \frac{r_1 / u'(r_1)^2 + r_2 / u'(r_2)^2}{1 / u'(r_1)^2 + 1 / u'(r_2)^2} \quad (18)$$

The standard uncertainty of  $r$  at the respective target pressure  $p_t$  is

$$u(r) = \sqrt{\left(\frac{u(p_{st,VNIIM})}{p_{st,VNIIM}}\right)^2 r^2 + \left(\frac{u(p_{st,UME})}{p_{st,UME}}\right)^2 r^2 + 2 \frac{(u_{T\sigma}(p_t))^2}{p_t^2} r^2 + \left(\frac{1}{u'^2(r_1)} + \frac{1}{u'^2(r_2)}\right)^{-1}} \quad (19)$$

The first two terms under the square root describe the influence of the uncertainty of the standard pressures  $p_{stj}$  that correlate to  $r_1$  and  $r_2$ , the third term is the uncertainty contribution due to the temperature dependence of  $\sigma_{eff}$  as described before Eq. (12), and the last term in the bracket is due to all other influences of Type A, which are due to the rotor instability, offset determination  $RD$ , temperature and scatter of data. Also for  $u_{T\sigma}$  it is conservatively assumed that  $r_1$  and  $r_2$  and respectively  $\sigma_{1j}$  and  $\sigma_{2j}$  are correlated by their temperature dependence of  $\sigma_{eff}$ .

The quantity

$$d = r - 1 \quad (20)$$

describes the relative difference between the two primary standards in this comparison, where

$$u(d) = u(r) \quad (21)$$

Equivalence is generally assumed if

$$d \leq 2u(d) = U(d) \quad (22)$$

or

$$|E_n| \leq 1 \quad (23)$$

with

$$E_n = \frac{d}{U(d)} \quad (24)$$

The values generated from Eqs. (20) to (24) are summarised in Table 11 below.

Table 11 Summary of data as a result of this comparison.  $r$  is the ratio of the true generated pressures in the two standards (Eq.(18)),  $d$  is the relative difference between the pressures in the two standards (Eq.(20)),  $U(d)$  is the expanded uncertainty ( $k=2$ ) of  $d$  (Eqs. (20), (21) and (22)) and  $E_n$  is defined by Eq. (24).

$P_t$ (Pa)	$r$	$d$	$U(d)$	$E_n$
3.0E-04	0.9115	-0.0885	0.0855	-1.04
9.0E-04	0.9589	-0.0411	0.0580	-0.71
3.0E-03	1.0312	0.0312	0.0299	1.04
9.0E-03	1.1206	0.1206	0.0374	3.22
3.0E-02	0.9885	-0.0115	0.0307	-0.37
9.0E-02	0.9930	-0.0070	0.0292	-0.24
3.0E-01	0.9929	-0.0071	0.0188	-0.38
9.0E-01	0.9950	-0.0050	0.0096	-0.52

## 12. Discussion and conclusions

The comparison has tested the degree of equivalence between the pressures generated at the primary vacuum standards of UME and VNIIM.

Some difficulties have encountered at the various stages of the comparison. Leaks were found in both primary vacuum standards. Leaks in two chambers were identified after the completion of the measurements in the first stage at UME, which was subsequently eliminated. They may have occurred after baking the UME primary standard. VNIIM identified a leak in the orifice flange that has been observed and eliminated immediately after having finished of the measurements. In addition, the transfer standard of UME during the first comparison at UME showed instability, so its results were eliminated and the standard was replaced by another. UME measurements less than  $9 \cdot 10^{-3}$  Pa in 2016 can be explained by a leak that was subsequently eliminated. The results confirm the major problem at VNIIM for the points  $3 \cdot 10^{-3}$  Pa and  $9 \cdot 10^{-3}$  Pa. A leak would have a greater effect at low pressures but not at intermediate pressures. Due to technical problems associated with both primary standards, fewer measurements were made than originally planned. Both primary vacuum standards were equivalent in the most part of the pressure range except for the target pressures  $3 \cdot 10^{-4}$  Pa,  $3 \cdot 10^{-3}$  and  $9 \cdot 10^{-3}$  Pa at the  $k=2$  level of expanded uncertainty.

The quality of the measurements does not allow a link to a corresponding CCM or EURAMET key comparison reference values and the results do not allow to support any CMC applications.

### 13. References

[1] Technical Protocol, COOMET.M.P-K15 Key Comparison for Absolute Pressure Between 0.3 mPa and 0.9 Pa

[2] Kangi R, Ongun B and Elkatmis A 2004 *Metrologia* 41 251–6

[3] Gorobei V N, Izrailov E K, Kuvandykov R E, Fomin D M and Chernyshenko A A 2018 IOP Conf. Ser.: Mater. Sci. Eng. 387

[4] Fremerey J. K. 1982 *Vacuum* 32 685–90

[5] Karl Jousten *et al* 2020 *Metrologia* 57 07031

[6] R Kacker and A Jones, On use of Bayesian statistics to make the “Guide to the expression of uncertainty in measurement” consistent, *Metrologia* 40 (2003), 235-248

[7] P A Carroll *et al*, NPL DEPC-EM 015 2007 Calibration of two Spinning Rotor Gauges as a bilateral comparison between NPL and INRIM in the range  $3 \cdot 10^{-4}$  Pa to  $9 \cdot 10^{-2}$  Pa

[8] K. Jousten, Is the effective accommodation coefficient of the spinning rotor gauge temperature dependant, *J.Vac.Sci. Technol. A* 21(1) (2003), 318-324.

[9] M.G.Cox, The evaluation of key comparison data, *Metrologia* 39 (2002), 589-595.

[10] K Jousten, Luis A Santander Romero and Jorge C. Torres Guzman, Final report on key Comparison SIM-EUROMET.M.P.BK3 (bilateral comparison) in the pressure range from  $3 \times 10^{-4}$  Pa to 0.9 Pa, *Metrologia* 42 No 1A (Technical Supplement 2005)